THE JOURNAL OF CHEMICAL PHYSICS **131**, 064302 (2009)

Time-dependent quantum wave-packet description of H and D atom tunneling in N–H and N–D photodissociation of methylamine and methylamine-d_2

Chen Levi,[1,a)] Ronnie Kosloff,[2] Yehuda Zeiri,[3] and Ilana Bar[1]
[1]*Department of Physics, Ben-Gurion University, Beer Sheva 84105, Israel*
[2]*Department of Physical Chemistry and the Fritz Haber Center for Molecular Dynamics, The Hebrew University of Jerusalem, Jerusalem 91904, Israel*
[3]*Department of Chemistry, Nuclear Research Center Negev, P.O. Box 9001, Beer Sheva 84190, Israel and Department of Biomedical Engineering, Ben-Gurion University, Beer Sheva 84105, Israel*

(Received 21 April 2009; accepted 22 July 2009; published online 12 August 2009)

The degree to which tunneling through a barrier in the N–H and N–D photodissociation channels of methylamine (CH_3NH_2) and its deuterated variant (CH_3ND_2), respectively, plays a role was investigated by time-dependent quantum wave-packet dynamics calculations. Two dimensional potential energy surfaces (PESs) of methylamine, presenting the N–H stretch and the HNC bend, were constructed employing multireference *ab initio* electronic-structure methods, allowing full description of the H motion on the $HC-NH_2$ plane. The time-dependent Schrödinger equation was solved employing the Fourier method for calculating the Hamiltonian operation together with the Chebychev polynomial expansion of the evolution operator. The results show that tunneling and decay to vibrational resonant states on the first excited electronic PES are faster for the H atom than for the D. The decay into two of the resonant states found on the first PES strongly depends on the initially excited vibrational state on the ground electronic PES. © *2009 American Institute of Physics*. [DOI: 10.1063/1.3204000]

I. INTRODUCTION

Time-dependent quantum mechanical calculations emerge as important tools for investigating molecular encounters and particularly absorption and breakup of molecules following photoexcitation. These studies are based on using calculated potential energy surfaces (PESs) with the molecule normally starting off in a single well defined quantum state, which then provides the specification for the initial wave packet in a very natural way.[1] Over the years, different molecules have been studied as exemplified by H_2O,[2–4] H_2S,[5] FNO,[6] O_3,[7] H_2O_2,[3] CH_3I,[8] CH_3ONO,[9] HCO,[10] HOCl,[11] and heteroaromatics including phenol[12] and pyrrole.[13] Most studies focused on small molecules, and studies on larger molecules such as the heteroaromatics used restricted dynamics in two collective coordinates to propagate the wave packet on the coupled surfaces.[12–14] In most cases the theoretical results could be compared to detailed experimental data, generating a detailed insight into the dissociation processes of the studied molecules.

An additional appealing system is the methylamine CH_3NH_2 molecule, which is the simplest primary amine, quite often appearing in organic and biologic building blocks. It is believed that studying the topography of its PESs and the dynamics may provide a better understanding of ultraviolet (UV) photoinduced processes in molecules containing amino moieties. Previous works by Kassab *et al.*[15] and Dunn and Morokuma[16] presented one dimensional PESs of the N–H, C–H, and C–N dissociation channels. Dunn and Morokuma[16] showed that there is a finite potential barrier of ~ 0.4 eV in the $\tilde{A}$ state along the N–H dissociation channel. Furthermore, their work also revealed single conical intersection (ci) points between the $\tilde{A}$ and the $\tilde{X}$ states along the N–H and C–N dissociation channels. Very recently we have shown[17] that the $\tilde{A}$ state includes a barrier along the N–H dissociation coordinate and that the $\tilde{X}$ and $\tilde{A}$ states are coupled by a line of ci, instead of a single point ci,[15,16] located in the $HC-NH_2$ plane. The existence of this line of ci was proven by the study of singularities in the (angular) nonadiabatic coupling terms and by finding the degeneracy points formed by the two interacting adiabatic PESs.

These theoretical studies[16,17] were triggered by previous experimental work. In particular, Waschewsky *et al.*[18] reported that excitation at 222 nm leads to N–H, C–N, and C–H rupture or H_2 elimination. By measuring the photofragment kinetic energies under collisionless conditions, they determined that C–N bond rupture proceeds on the excited state surface, while N–H rupture occurs via a ci, resulting in ground state products. Additional studies focused only on the H and D channels resulting from the UV dissociation of methylamine and its deuterated isotopologues.[19–23] Ashfold and co-workers[19,20] studied the photodissociation of four methylamine isotopologues (CH_3NH_2, CD_3NH_2, CH_3ND_2, and CD_3ND_2) at several wavelengths in the 203.0–236.2 nm range using the high resolution H(D)-atom Rydberg tagging. These studies[19,20] suggested a dominant role for the N–H(D) fission, where at least two dissociation pathways lead to

---

[a)] Electronic mail: chenle@bgu.ac.il.

0021-9606/2009/131(6)/064302/7/$25.00

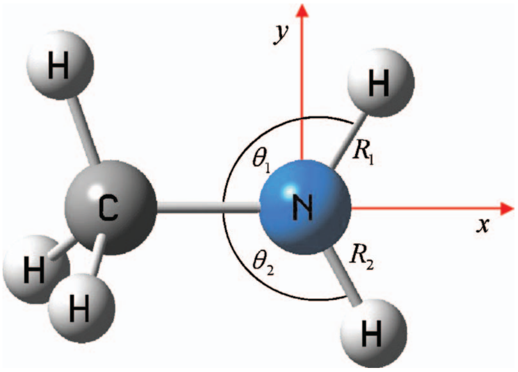

FIG. 1. The equilibrium structure of methylamine with five atoms, namely, carbon, nitrogen, two amine hydrogens, and a methyl hydrogen assumed to form a fixed plane (the HC–NH_2 plane). The θ_1 and R_1 coordinates were varied to form the PESs, which were then transformed to the x and y Cartesian coordinates.

H(D) atom fragments: The first corresponding to "dynamical" (high) total kinetic energy release and the second to "statistical" (slower) H atoms. Support to photodissociation via tunneling followed by a radiationless transition to the ground state was also obtained from the studies of vibrationally excited molecules.[21,22]

The experimental work by Kim and co-workers[24] gave further support to the theoretical finding[16] that a barrier exists along the N–H channel. In this work $(1+1)$ resonance enhanced multiphoton ionization in the $41\,500-44\,000\ \text{cm}^{-1}$ region was used to ionize the CH_3NH_2 and CH_3ND_2 molecules. They saw significant differences in the linewidths of the two molecules, implying that the lifetimes of the rovibrational levels on the first excited electronic state $\tilde{A}$ of CH_3NH_2 were significantly shorter (by an order of magnitude) than those of CH_3ND_2. Since an exponential relation to the mass was found, this difference between the two molecules and the large H/D isotope effect were attributed to the tunneling through the potential barrier along the N–H channel.[16] Very recently we have shown[25] that the dissociation probability of the hydrogen atoms released from methylamine increases extensively by promoting the molecule to excited vibrational states on the first bound electronic state. By comparing the experimental data to an analytical model and to dynamical calculations, we have shown that this behavior is consistent with a dissociation process dominated by tunneling.

In this paper we focus on the time-dependent quantum wave-packet dynamics study of methylamine and its deuterated isotopologue, methylamine-d_2 (CH_3ND_2), allowing to establish the degree to which tunneling through a barrier in the respective N–H and N–D dissociation channels plays a role. We study the wave-packet propagation from different initial conditions and the decay of the wave packets to resonant vibrational states, as well as the time scales for these processes.

II. THEORETICAL FRAMEWORK

In what follows the triatomic amine group is assumed to form a plane with one of the HC diatoms in the methyl group (see Fig. 1). Two dimensional PESs for the ground $^1A'$ and the first excited $^1A''$ electronic states were calculated. The two degrees of freedom chosen were the N–H stretch (R_1) and the HNC bend (θ_1) which allow full description of the H motion on the HC–NH_2 plane. The PESs were calculated using the MOLPRO (Ref. 26) package with the multireference configuration interaction (MRCI) method and the 6-31+G* basis set. We used an active space including two valence electrons distributed among five orbitals (three of them belonging to the A' irreducible representation). The two-dimensional diabatic PESs are presented in Fig. 2 in terms of Cartesian coordinates $(x,y)=[R_1\cos(\pi-\theta_1),R_1\sin(\pi-\theta_1)]$ and with the origin located on the nitrogen atom (see Fig. 1). At this point, it is important to point out that all the calculations presented below were performed with these diabatic PESs.

The H motion in the HC–NH_2 plane was done by a two dimensional direct dynamics calculation, carried out by a code written in MATLAB 7.0 (Ref. 27) and based on a numerical algorithm introduced by Kosloff and co-workers.[28–32]

Briefly, in quantum mechanics the time evolution is governed by the time-dependent Schrödinger equation

$$\hat{H}\psi = i\hbar\frac{\partial}{\partial t}\psi, \tag{1}$$

where $\hat{H}$ is the Hamiltonian operator. In order to carry out the numerical calculations of the system dynamics, the wave function is discretized on the same grid points as the PES. Next, solving $\hat{H}\psi$ is performed in two parts, where the potential part is evaluated simply by calculating the scalar product $U\psi$ (U is the PES), and the kinetic part which is somewhat more complicated, due to the fact that the kinetic operator is nonlocal in a different manner. The nonlocalization problem can be solved by using the Fourier method in which the action of the kinetic energy operator is calculated

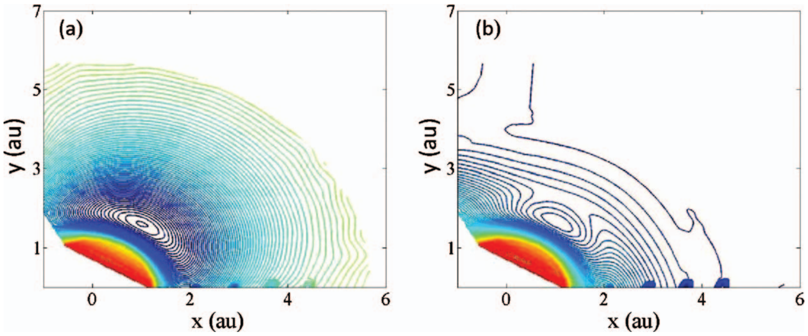

FIG. 2. The two dimensional diabatic PESs in terms of Cartesian coordinates $(x,y)=[R_1\cos(\pi-\theta_1),R_1\sin(\pi-\theta_1)]$. The origin of the coordinates is located at the nitrogen atom (see Fig. 1). (a) The ground surface. (b) The first excited electronic state surface.

TABLE I. Energy eigenvalues of the seven lowest vibrational states on the PES of the ground electronic state and their quantum number assignments.

CH_3NH_2		CH_3ND_2	
E_n (cm^{-1})	(n_1,n_2)	E_n (cm^{-1})	(n_1,n_2)
2794	(0,0)	1964	(0,0)
4242	(0,1)	2991	(0,1)
5672	(0,2)	4013	(0,2)
6507	(1,0)	4657	(1,0)
7081	(0,3)	5027	(0,3)
7956	(1,1)	5735	(1,1)
8442	(0,4)	5962	(0,4)

in the momentum space. The discrete Fourier transform is used in order to get the momentum-space-wave function, then this wave function is multiplied by $-\hbar^2 k^2$ and the inverse discrete Fourier transform is applied to return to configuration space.

The general solution of the time-dependent Schrödinger equation [Eq. (1)] is

$$\psi(t+dt) = e^{-i(\hat{H}/\hbar)dt}\psi(t), \qquad (2)$$

where the term $e^{-i(\hat{H}/\hbar)dt}$ is called the evolution operator. To solve Eq. (2), the evolution operator is expanded in a series of complex Chebychev polynomials,

$$e^{-i(\hat{H}/\hbar)dt} \approx \sum_{n=o}^{N} a_n \varphi_n\left(-i\frac{\hat{H}}{\hbar}dt\right), \qquad (3)$$

where φ_n are the complex Chebychev polynomials and a_n are the expansion coefficients based on the Bessel functions of the first kind (the $\approx$ sign is due to the finite value of the employed terms).

The use of the Fourier method to calculate the kinetic energy implies periodic boundary conditions, which cause spurious behavior that needs to be eliminated. Therefore, we added a complex absorbing potential to the PESs in the range $R_1 = 3-6$ Å to eliminate these boundary effects.[33,34]

The evolution operator was first used to propagate the wave packet with imaginary time in order to generate the vibrational eigenstates on the ground state diabatic PES. The eigenstates were then used as the initial wave packets for the propagation on the excited diabatic electronic state. The lifetimes of the vibrational resonance states on the excited state were evaluated from the imaginary part of the energy expectation value[35–37]

$$E_{res} = E_r - i\frac{\tau}{2}, \qquad (4)$$

where E_r and τ are the energy and lifetime of the resonance, respectively.

III. RESULTS AND DISCUSSION

Figure 2 displays the two dimensional diabatic PESs in terms of Cartesian coordinates $(x,y)=[R_1 \cos(\pi-\theta_1), R_1 \sin(\pi-\theta_1)]$, where the coordinates' origin is located at the nitrogen atom (see Fig. 1). Inspection of Fig. 2 shows

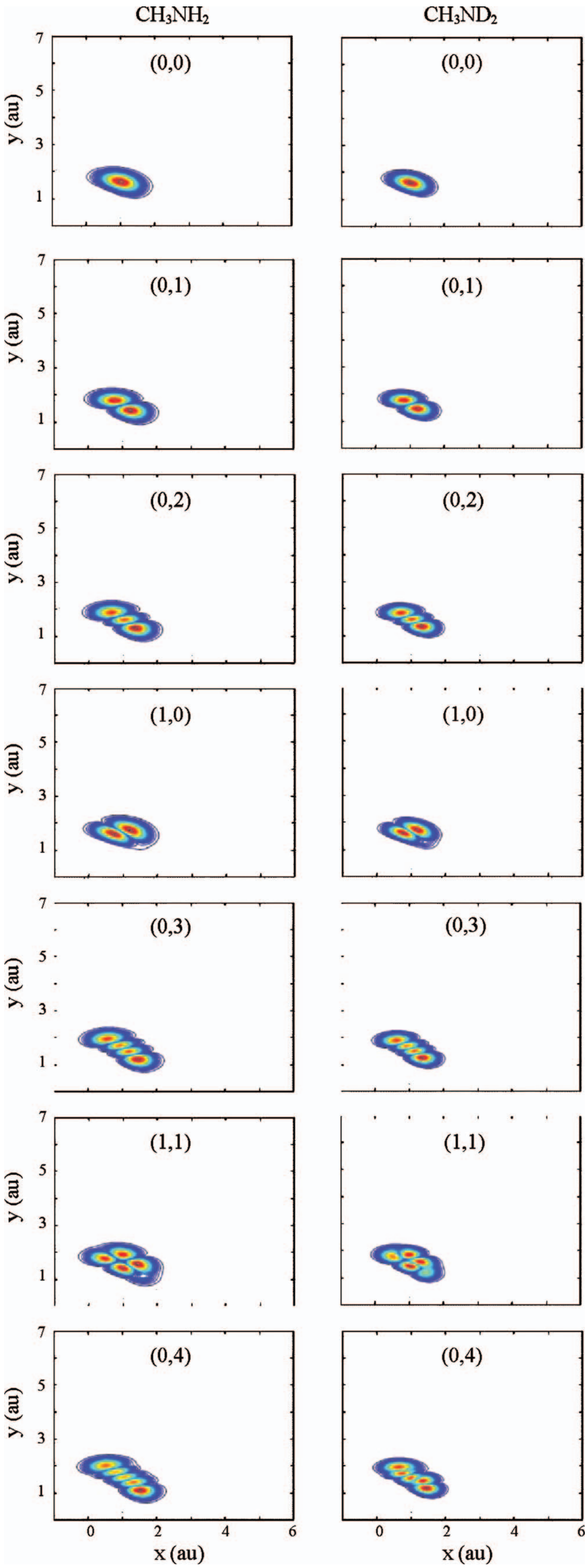

FIG. 3. Contour maps in the x-y space (see Fig. 2) presenting the probability densities of the energy eigenvalues of the lowest vibrational states on the ground PESs for methylamine and methylamine-d_2. The notations (n_1,n_2) relate to the quantum numbers of the N–H (N–D) stretch and the CNH (CND) bend, respectively.

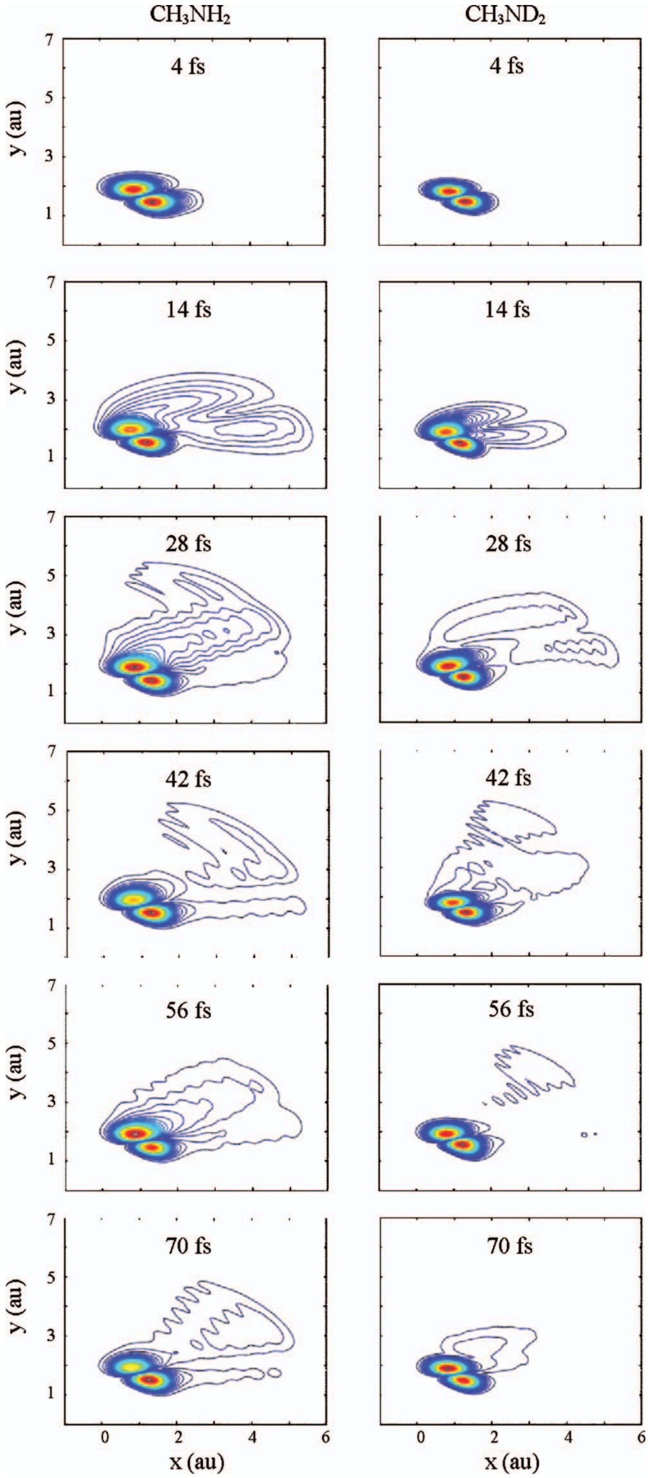

FIG. 4. Contour maps in the x-y space (see Fig. 2) presenting the propagation of the wave packet from the (0,1) initial vibrational state. The wave packet maintains the two node form. The CH_3NH_2 molecule is resonating with a time period of ~28 fs, while the CH_3ND_2 with ~40 fs, taking longer for that phenomenon to be notable.

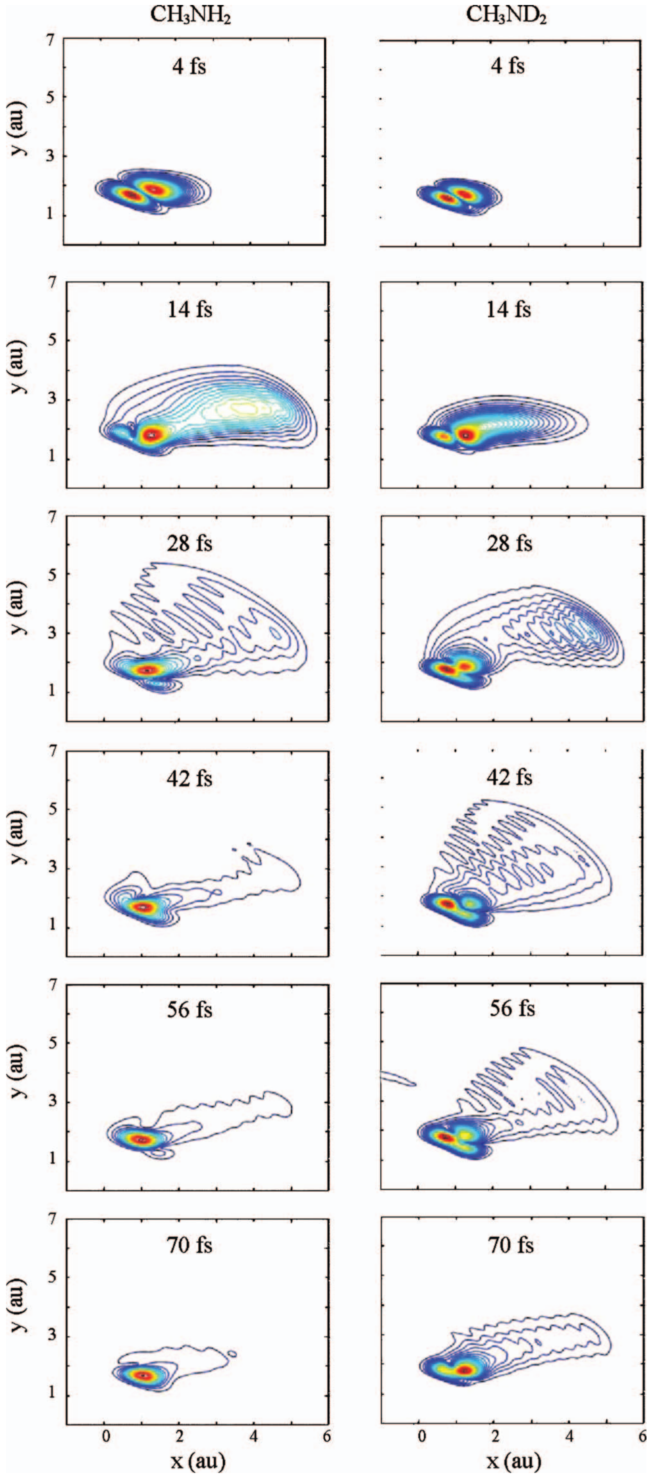

FIG. 5. Contour maps in the x-y space (see Fig. 2) presenting the propagation of the wave packet from the (1,0) initial vibrational state of CH_3NH_2 and CH_3ND_2. The wave packet decays very quickly to a single node formation.

a bound excited electronic state with a small potential barrier of ~0.016 hartree followed by a crossing with the ground electronic state. The excited PES after the barrier is essentially a repulsive one.

Table I presents the energy eigenvalues of the lowest vibrational states on the ground PES and their quantum number assignments. The probability densities of the corresponding states (i.e., the absolute values of the wave functions) are shown in Fig. 3. The notations n_1 and n_2 relate to the quantum numbers of the N–H (N–D) stretch and the CNH (CND) bend, respectively. The fundamental frequencies for the N–H and N–D stretches on the ground electronic states are 3712 and 2693 cm^{-1}, where the corresponding experimental values[38–40] [average of the NH_2 (ND_2) symmetric and antisymmetric stretches] are 3392 and 2518 cm^{-1}. The funda-

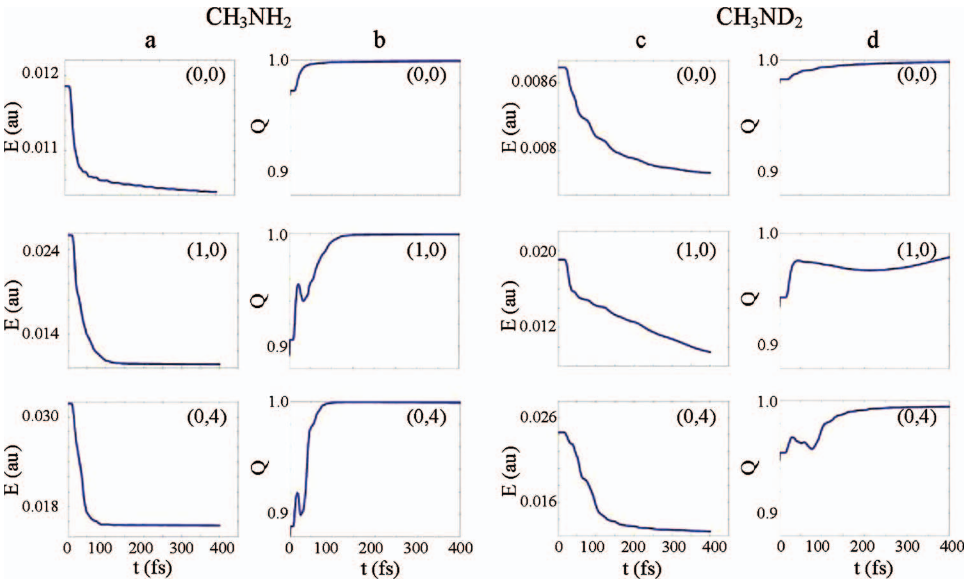

FIG. 6. The energies and overlapping parameters as a function of time for the (0,0), (1,0), and (0,4) initial states: (a) the CH_3NH_2 energies, (b) the CH_3NH_2 overlapping parameters, (c) the CH_3ND_2 energies, and (d) the CH_3ND_2 overlapping parameters.

mental frequencies for the CNH and CND bends are 1448 and 1027 cm^{-1}, where the corresponding experimental values[38–40] [averaging the NH_2 (ND_2) scis and twist] are 1474 and 1027 cm^{-1}. These calculated fundamental frequencies match well with the experimental values and were therefore used as the initial vibrational states for wave-packet propagation.

The time evolution of the wave packets from the (0,1) and (1,0) initial states is shown in Figs. 4 and 5, respectively. The figures show the part of the wave packet that remained on the excited PES at the specified time, not including the part that already dissociated. While the (0,1) state maintained the two node form, the (1,0) state decayed very quickly to a single node formation. Also visible in these figures is the fact that the CH_3NH_2 evolution is much faster than that of CH_3ND_2. For the CH_3NH_2 molecule with the (0,1) initial state (left column in Fig. 4), it is clear that the part of the wave packet that remains in the potential well during propagation is resonating. The resonance time period for CH_3NH_2 is ~28 fs (panels for 14, 42, and 70 fs and for 28 and 56 fs, respectively, are similar). Similar situation occurs in the CH_3ND_2 with a resonance time of ~40 fs; however, it took about 80 fs until the wave packet decayed enough so that the resonance could be notable.

To obtain a better understanding of the single versus double node resonances, the calculations were repeated while keeping the wave packet normalized at all time. By doing so, the system reaches a steady state in which continuous flux (via tunneling) leads to dissociation while the part of the wave packet that stays in the potential well reaches a resonant state. The criteria for convergence to the steady state can be obtained from two parameters. The first is simply the convergence of the system energy. For the second, a new variable is defined, $O(t)=|\langle\psi(t)|\psi(t-1)\rangle|$, which is the overlap between two subsequent wave packets. The convergence is reached as the overlap parameter approaches 1.

Figure 6 presents the time evolution of the energy and the overlap parameters for the (0,0), (1,0), and (0,4) initial states. Columns a and c present the energies of CH_3NH_2 and CH_3ND_2, respectively, while columns b and d show the variation in the overlap parameters. It is clear, in all shown cases, that the CH_3NH_2 decayed much faster than the CH_3ND_2. For instance, the (0,4) initial state reached convergence within ~50 fs for CH_3NH_2 and about three times slower for the CH_3ND_2. For the (0,0) and (1,0) states, the differences in convergence times are even larger. These differences are due to two reasons: The first is the mass difference between the H and D atoms, which causes the tunneling process to be much slower for the latter, and the second is that the CH_3ND_2 initial vibrational states are lower in energy by a factor of $\sqrt{2}$ (see Table I) due to differences in reduced masses. Also notable in Fig. 6 is that the (0,4) state exhibits the fastest decay (for both molecules) while the (0,0) is the slowest one, indicating a faster decay for larger initial energy. This is reasonable since higher energy of the accessed vibrational state on the excited PES leads to faster tunneling. This finding is in line with our very recent[25] results which have shown increased hydrogen atom release as the methylamine molecule was promoted to higher excited vibrational states on the first bound electronic state. This behavior was attributed to increased tunneling probability as higher excited states were accessed.

It is interesting to note that after propagating the wave packets for 400 fs (while keeping them normalized all the time) all the different initial states decayed to single or double node resonances. The (0,0) and (1,0) initial states decayed to a single node resonance with energies of 2260 and 1669 cm^{-1} for CH_3NH_2 and CH_3ND_2, respectively. All other initial states [(0,1), (0,2), (0,3), (1,1), and (0,4)] involving excitation of CNH and CND bends decayed to a double node resonance with energies of 3390 and 2489 cm^{-1}. The lifetimes of these resonant states, obtained from the imaginary part of the energy, were found to be 1.2 and 13.4 ps for the single node resonances of CH_3NH_2 and CH_3ND_2, respectively, and much shorter for the double node resonances, i.e., 0.2 and 3.0 ps. These calculated lifetimes show a similar behavior as the experimental results of Kim and co-workers.[24] Their analysis of the spectral linewidths showed that the lifetime of $CH_3NH_2(\widetilde{A})$ is $\tau \sim 0.38$ ps at the origin band, compared to ~8.8 ps for CH_3ND_2 $(\widetilde{A})$, implying a ratio of ~23 between the two lifetimes compared to a ratio of ~12 in our calculation.

The wave packets of all seven initial states following 400 fs propagation are shown in Fig. 7. It is clearly seen that all initial states decayed to the same double nodes resonance (with similar energy), except the (0,0) and (1,0) states which both decayed to the same single node resonance.

IV. CONCLUSIONS

This work focused on the tunneling of the H and D atoms during bond fission of the N–H and N–D bonds in photoexcited CH_3NH_2 and CH_3ND_2 molecules, respectively. Results corresponding to a two dimensional model, including the N–H stretch (reaction coordinate) and the CNH bend, were obtained for restricted motion of the H (D) atom on the $HC-NH_2$ plane. The model is based on the solution of the time-dependent Schrödinger equation obtained by a combination of the Fourier and the Chebychev methods.

The two dimensional PESs of the ground and first excited electronic states were calculated using the MRCI method. Time-dependent quantum dynamics was used to propagate the wave packets with imaginary time to calculate the eigenvalues of the seven lowest vibrational states on the ground electronic state and to assign them to the quantum numbers of the N–H (N–D) stretches and the CNH (CND) bends. The fundamental frequencies of the calculations agree well with the experimental values. The calculated eigenvalues were used as initial states and allowed to propagate (in time) on the excited state PES to study the tunneling process and the decay to resonant vibrational states. Eventually, we repeated the propagations, keeping the wave packets normalized, to achieve conversion to a steady state.

The results showed faster tunneling and decay to resonant states for CH_3NH_2 than for CH_3ND_2, where the time scale for tunneling was found to be dependent on the initial vibrational state. States with higher energy resulted in faster processes. Two resonant states were found on the excited PES and their energies and lifetimes were calculated. It was found that all the examined initial states eventually decayed to one of these two states. The initial states (0,0) and (1,0) of the CH_3NH_2 molecule decayed to the lowest resonant state with energy of 2260 cm^{-1} and lifetime of 1.2 ps and the corresponding CH_3ND_2 states to the resonant state with energy of 1669 cm^{-1} and 13.4 ps lifetime. On the other hand, initial states involving the CNH (CND) bends [(0,1), (0,2), (0,3), (1,1), and (0,4)] decayed to resonant states with higher energy of 3390 cm^{-1} and shorter lifetime of 0.2 ps for the CH_3NH_2 molecule and 2489 cm^{-1} and 3.0 ps for the CH_3ND_2.

The results obtained in the two dimensional direct dynamics calculations open a window to the understanding of the tunneling process occurring during the N–H (N–D) dissociation process, showing a strong dependence on the initial vibrational states. However, this study neglected intramolecular vibrational redistribution arising from anharmonic coupling of the initially prepared mode with other vibrational

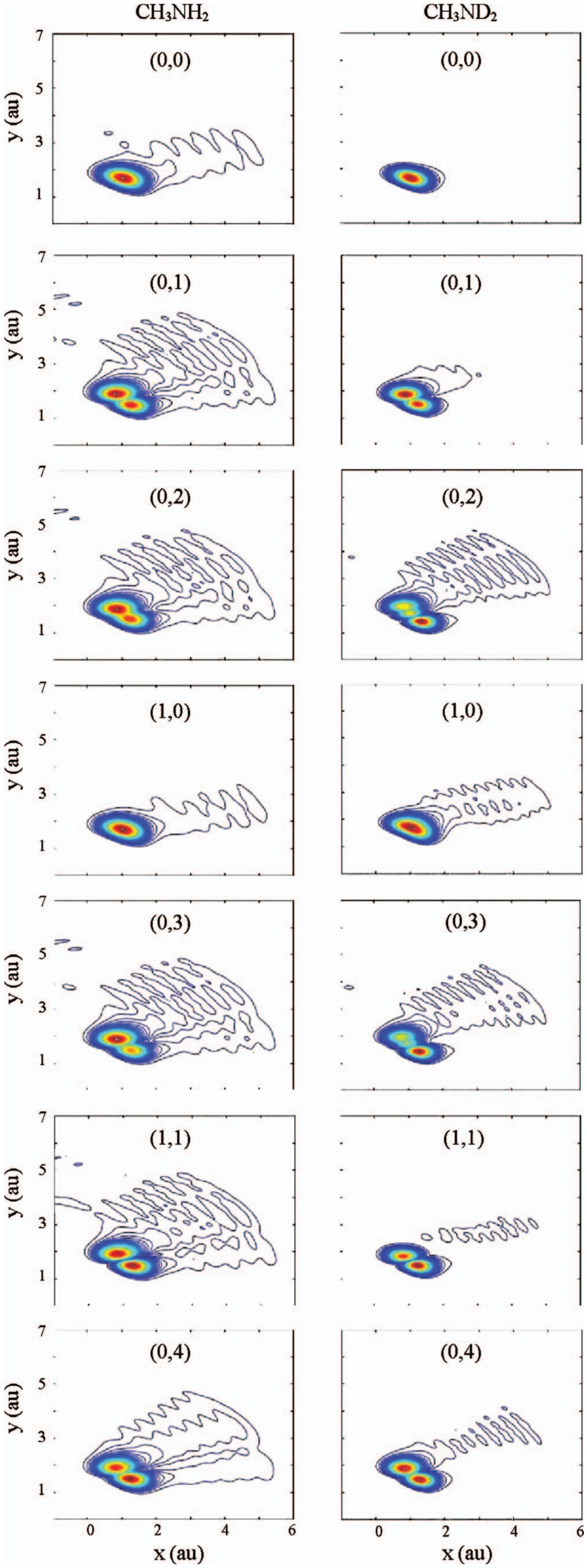

FIG. 7. Contour maps in the *x*-*y* space (see Fig. 2) presenting the wave packets (kept normalized during all time) following 400 fs propagation. All the initial states decayed to the same double node resonance (with similar energy), except the (0,0) and (1,0) states which both decayed to the same single node resonance.

degrees of freedom. Therefore, we believe it will be very interesting to extend the present study to test this issue as well as to higher dimensionality studies including more of the possibly participating degrees of freedom.

ACKNOWLEDGMENTS

Financial support from the Israel Science Foundation founded by The Israel Academy of Science and Humanities and the James Franck Binational German-Israeli Program in Laser-Matter Interaction is gratefully acknowledged.

[1] G. G. Balint-Kurti, Int. Rev. Phys. Chem. **27**, 507 (2008) (and references therein).

[2] J. Zhang and D. G. Imre, J. Chem. Phys. **90**, 1666 (1989); D. G. Imre and J. Zhang, Chem. Phys. **139**, 89 (1989).

[3] K. Kuhl and R. Schinke, Chem. Phys. Lett. **158**, 81 (1989).

[4] K. Weide and R. Schinke, J. Chem. Phys. **90**, 7150 (1989).

[5] R. N. Dixon, C. C. Marston, and G. G. Balint-Kurti, J. Chem. Phys. **93**, 6520 (1990).

[6] H. U. Suter, J. R. Huber, M. von Dirke, A. Untch, and R. Schinke, J. Chem. Phys. **96**, 6727 (1992).

[7] D. Chasman, D. J. Tannor, and D. G. Imre, J. Chem. Phys. **89**, 6667 (1988).

[8] A. D. Hammerich, U. Manthe, R. Kosloff, H.-D. Meyer, and L. S. Cederbaum, J. Chem. Phys. **101**, 5623 (1994).

[9] R. Schinke, S. Hennig, A. Untch, M. Nonella, and J. R. Huber, J. Chem. Phys. **91**, 2016 (1989).

[10] A. Loettgers, A. Untch, H.-M. Keller, R. Schinke, H.-J. Werner, C. Bauer, and P. Rosmus, J. Chem. Phys. **106**, 3186 (1997).

[11] H. Guo, J. Phys. Chem. **97**, 2602 (1993).

[12] Z. Lan, W. Domcke, V. Vallet, A. L. Sobolewski, and S. Mahapatra, J. Chem. Phys. **122**, 224315 (2005).

[13] V. Vallet, Z. Lan, S. Mahapatra, A. L. Sobolewski, and W. Domcke, J. Chem. Phys. **123**, 144307 (2005); Faraday Discuss. **127**, 283 (2004); Z. Lan, A. Dupays, V. Vallet, S. Mahapatra, and W. Domcke, J. Photochem. Photobiol., A **190**, 177 (2007).

[14] D. Feit, J. A. Fleck, and A. Steiger, J. Comput. Phys. **47**, 412 (1982).

[15] E. Kassab, J. T. Gleghorn, and E. M. Evleth, J. Am. Chem. Soc. **105**, 1746 (1983).

[16] K. M. Dunn and K. Morokuma, J. Phys. Chem. **100**, 123 (1996).

[17] C. Levi, G. J. Halász, Á. Vibók, I. Bar, Y. Zeiri, R. Kosloff, and M. Baer, J. Chem. Phys. **128**, 244302 (2008); Int. J. Quantum Chem. **109**, 2482 (2009); J. Phys. Chem. A **113**, 6756 (2009).

[18] G. C. G. Waschewsky, D. C. Kitchen, P. W. Browning, and L. J. Butler, J. Phys. Chem. **99**, 2635 (1995).

[19] M. N. R. Ashfold, R. N. Dixon, M. Kono, D. H. Mordaunt, and C. L. Reed, Philos. Trans. R. Soc. London, Ser. A **355**, 1659 (1997).

[20] C. L. Reed, M. Kono, and M. N. R. Ashfold, J. Chem. Soc., Faraday Trans. **92**, 4897 (1996).

[21] A. Golan, S. Rosenwaks, and I. Bar, J. Chem. Phys. **125**, 151103 (2006); Isr. J. Chem. **47**, 11 (2007); A. Golan, A. Portnov, S. Rosenwaks, and I. Bar, Phys. Scr. **76**, C79 (2007).

[22] R. Marom, U. Zecharia, S. Rosenwaks, and I. Bar, Chem. Phys. Lett. **440**, 194 (2007); Mol. Phys. **106**, 213 (2008); J. Chem. Phys. **128**, 154319 (2008).

[23] D.-S. Ahn, J. Lee, J.-M. Choi, K.-S. Lee, S. J. Baek, K. Lee, K.-K. Baeck, and S. K. Kim, J. Chem. Phys. **128**, 224305 (2008).

[24] S. J. Baek, K.-W. Choi, Y. S. Choi, and S. K. Kim, J. Chem. Phys. **117**, 10057 (2002); **118**, 11026 (2003); M. H. Park, K. W. Choi, S. Choi, S. K. Kim, and Y. S. Choi, *ibid.* **125**, 084311 (2006).

[25] *Quantum tunneling of hydrogen atom in dissociation of photoexcited methylamine*, R. Marom, C. Levi, T. Weiss, S. Rosenwaks, Y. Zeiri, R. Kosloff, and I. Bar (unpublished).

[26] MOLPRO, a package of *ab initio* programs designed by H.-J. Werner and P. J. Knowles, R. Lindh, F. R. Manby, M. Schütz *et al.*

[27] MATLAB 7.0.0.19920 (R14), The MathWorks, Inc., 2004.

[28] R. Kosloff, *Dynamics of Molecules and Chemical Reactions* (Marcel Dekker, New York, 1996), p. 185.

[29] D. Kosloff and R. Kosloff, J. Comput. Phys. **52**, 35 (1983).

[30] H. Tal-Ezer and R. Kosloff, J. Chem. Phys. **81**, 3967 (1984).

[31] R. Kosloff, J. Phys. Chem. **92**, 2087 (1988).

[32] R. Baer, Y. Zeiri, and R. Kosloff, Phys. Rev. B **54**, R5287 (1996).

[33] R. Kosloff and D. Kosloff, J. Comput. Phys. **63**, 363 (1986).

[34] D. Neuhasuer and M. Baer, J. Chem. Phys. **90**, 4351 (1989).

[35] T. Berggren and P. Olanders, Nucl. Phys. A **473**, 189 (1987).

[36] N. Moiseyev and U. Peskin, Phys. Rev. A **42**, 255 (1990).

[37] H. Masui, S. Aoyama, T. Myo, and K. Katō, Prog. Theor. Phys. **102**, 1119 (1999).

[38] A. P. Gray and R. C. Lord, J. Chem. Phys. **26**, 690 (1957).

[39] J. R. Durig and C. Zheng, Struct. Chem. **12**, 137 (2001).

[40] Y. Hamada, N. Tanaka, Y. Sugawara, A. Y. Hirakawa, M. Tsuboi, S. Kato, and K. Morokuma, J. Mol. Spectrosc. **96**, 313 (1982).